

Novel Photoinduced Recovery of OFET Memories Based on Ambipolar Polymer Electret for Photorecorder Application

Chia-Hui Chen, Yang Wang, Hiroki Tatsumi, Tsuyoshi Michinobu,* Shu-Wei Chang, Yu-Cheng Chiu,* and Guey-Sheng Liou*

A new design concept for novel photoresponsive flash organic field-effect transistor (OFET) memory is demonstrated by employing the carbazole-dioxazine polymer (Poly CD) as an electret. Photoactive electrets that can absorb the light effectively rather than photoactive semiconductors are proposed by the “photoinduced recovery” mechanism in the literature; however, the correlation between the chemical structure and photoresponsive electrical performances is ambiguous. In this study, it is reported for the first time that the OFET memory with trapped charges can be optically recovered by a polymer electret and the working mechanism can be explained by the structural design. The highly planar Poly CD electret exhibits photoluminescence quenching in film states, resulting in the generation of sufficient excitons to eliminate trapped charges under light excitation. Additionally, the Poly CD electret with coplanar donor–acceptor moieties is suitable for both p-channel and n-channel semiconductors. For p-type memory devices, a large memory window (82 V) and stable nonvolatile retention performance with high ON/OFF ratio could be obtained. The memories also display good switching reliability for voltage-programming and light-erasing cycles. This study provides useful information for the development of polymer-based photoresponsive flash OFET memories and demonstrates the practical applications of photorecorder and photosensitive smart tag.

1. Introduction

Organic field effect transistor (OFET) memory devices have attracted considerable attention as a promising candidate for next-generation data storage electronics due to the properties of nondestructive read-out and compatibility with integrated

circuits even on soft substrates.^[1] Different from conventional OFETs, the OFET memory is integrated with a functionally chargeable electret layer between the semiconductor and dielectric layer. The chargeable electrets with the ability of storing charge could be generally categorized into ferroelectrically oriented dipole-dielectric materials,^[2] nanofloating gate,^[3] and polymeric charge trapping materials.^[1b,4] The channel conductance would be tuned by the different polarized state of electrets upon programming or erasing operation, modulated by electrical stress to inject or release charges.

To date, with the rapid progress, numerous research studies have indicated that light could also be utilized as the impetus to fully or partially substitute for electrical operation.^[5] Light-operating memories possess remarkable advantages regarding energy savings, efficient elimination of data for rewritable properties, and extended application as a photosensor. However, the detective wavelength of the common organic semiconductors is limited in visible light region, such as pentacene.^[5a,6] As a result, a modified


electret with the capability of tunable emission wavelength is necessary to overlap the absorption of pentacene, which is an inefficient method due to the indirect absorption from incident light.^[7] Recently, in the field of inorganic electronics, 2D materials with van der Waals heterostructure are emerging due to the photoelectric properties, and it allows for flexible

C.-H. Chen, Prof. G.-S. Liou
Institute of Polymer Science and Engineering
National Taiwan University
No. 1, Sec. 4, Roosevelt Road, Taipei 10617, Taiwan
E-mail: gsliau@ntu.edu.tw

Dr. Y. Wang, H. Tatsumi, Prof. T. Michinobu
Department of Materials Science and Engineering
Tokyo Institute of Technology
2-12-1 Ookayama, Meguro-ku, Tokyo 152-8552, Japan
E-mail: michinobu.t.aa@m.titech.ac.jp

S.-W. Chang, Prof. Y.-C. Chiu
Department of Chemical Engineering
National Taiwan University of Science and Technology
No. 43, Sec. 4, Keelung Rd., Da'an Dist., Taipei City 10607, Taiwan
E-mail: ycchiu@mail.ntust.edu.tw

Prof. Y.-C. Chiu, Prof. G.-S. Liou
Advanced Research Center for Green Materials Science and Technology
National Taiwan University
Taipei 10617, Taiwan

 The ORCID identification number(s) for the author(s) of this article can be found under <https://doi.org/10.1002/adfm.201902991>.

DOI: 10.1002/adfm.201902991

electronic application as well. However, the device fabrication often requires multistep processes, limiting their potential in large-area production by using standard processing methods.^[8] To overcome the limitation of semiconductor absorption, some photoactive particles, such as C₆₀ molecules and CdSe quantum dots, were added to the electrets in floating gate configuration.^[9] After the light illumination, the light-erasing process occurred, which was mainly attributed to the exciton generation from the photoactive moieties, and the phenomenon has been proposed in a “photoinduced recovery” mechanism. Nevertheless, the preparation process of quantum dots with surface modification for enhancing dispersity in the floating-gate film complicated the device fabrication. In addition, the guideline of strategy for designing light-erasable memory devices is still ambiguous.

Therefore, we first proposed the light-erasable memory devices with easily processable polymeric electrets by elaborating the “photoinduced recovery” mechanism. From the viewpoint of the electret chemical structure, a photoactive carbazolidioxazine-based polymer (Poly CD) was designed to form light-erasable OFET memories. Poly CD was composed of the electron-donating carbazole moiety and electron-accepting dioxazine family in the coplanar fused ring framework, which enable to capture both positive and negative charges in p-type and n-type channel devices, respectively. Furthermore, the Poly CD in thin-film state exhibited an aggregation-caused quenching (ACQ) property, and thus the conjugated structure in the major part (CD segment) could effectively generate excitons to eliminate the trapped carriers.^[10] Note that the OFET memory devices exhibited nonerasable properties under the electrical operating mode. However, after the light illuminating, the devices showed photoinduced recovery behavior no matter what the p-type or n-type. For the consideration of retention properties, fully conjugated structures should be avoided, because the stored charges would be dissipated by conductive route.^[11] Thus, for chemical structure design, the major part (CD segment) responsible for memory characteristics was connected by bisphenol A with a soft ether linkage in order to

perturb the stacking. In this way, the p-type OFET memories showed good reliability with the retention time for 10⁴ s and the high memory ON/OFF ratio over three orders of magnitude. The design also successfully reflected the durability test where the voltage-driven programming and light-driven erasing could be continuously carried out over 100 times without obvious decay. Finally, the novel photoinduced recovery OFET memory could serve as an excellent candidate for the application to a photorecorder.

2. Results and Discussion

2.1. Synthesis of Carbazolidioxazine Derivatives (CD)

The synthetic route of Poly CD is shown in **Figure 1**. Fluorinated CD was synthesized according to a reported procedure.^[12] Due to the branched 2-decyltetradecyl groups, CD was sufficiently soluble in common polar solvents. Accordingly, aromatic nucleophilic substitution polymerization with bisphenol A was attempted. A mixture of CD and bisphenol A in NMP was heated to 180 °C for 20 h in the presence of K₂CO₃. The crude product was washed with methanol in a Soxhlet extractor, yielding the corresponding Poly CD in 46% yield. Proton nuclear magnetic resonance (¹H NMR) spectrum of this polymer was very broad, but the peaks were ascribed to the CD and bisphenol A monomer units, suggesting the absence of any noticeable side reactions (Figure S1, Supporting Information). The weight-average molecular weight (*M_w*) and polydispersity (*M_w*/*M_n*), determined by gel permeation chromatography (GPC) with tetrahydrofuran (THF) as an eluent at 40 °C, were 4000 and 1.2, respectively.

2.2. p-Type OFET Memory Employing Poly CD Based Electret

The p-type pentacene based OFET memory devices constructed with Poly CD electrets were fabricated on SiO₂/Si substrates

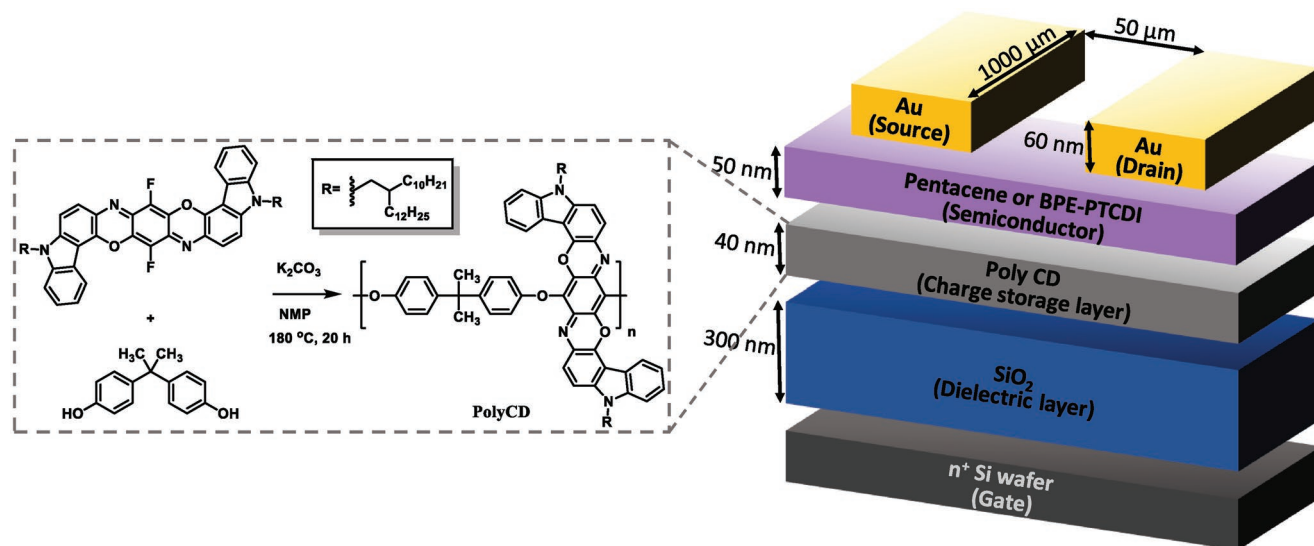


Figure 1. Synthesis of Poly CD and the schematic configuration of Poly CD based OFET memory devices.

in a bottom-gate/top-contact configuration, as illustrated in Figure 1. The surface morphology of the electret film analyzed by atomic force microscopy (AFM) presented a very smooth and uniform image with a low root-mean-square (RMS) roughness value below 1 nm, as shown in Figure S2a (Supporting Information), which could promote the growth and crystallinity of overlying organic semiconductors and reduce the amount of interface traps between the semiconductor and electret layers. In addition, the Poly CD film possessed hydrophobic nature with a water contact angle of 100° (Figure S2c, Supporting Information), indicating that the properties of low surface energy improved the wettability of pentacene on the smooth electret surface.^[13] As a result, Poly CD could offer a beneficial environment to deposit well-growth pentacene (Figure S2b, Supporting Information).

The electrical transfer and output characteristics of the p-type Poly CD based OFET memory devices are shown in Figures S3 and S4 (Supporting Information), respectively. All the measurements were conducted in a truly dark environment except for optical operation. The transfer curves exhibited a typical p-type accumulation mode with a good current modulation. However, the Poly CD based devices showed relatively low saturation drain current and mobility, due to the superior hole-trapping ability that could withdraw the mobile positive carriers from the conductive channel.^[14] While the source-drain voltage (V_d) is fixed at -60 V, the device exhibited a high ON/OFF current ratio of 10^5 – 10^6 and a quite low threshold voltage around 0 V.

To further investigate the memory characteristics of the p-type Poly CD based OFET memory devices, appropriate gate pulses (V_g) were exerted on the devices for programming or erasing purposes. All transfer curves were measured under a fixed drain voltage of -60 V. After negative gate biases were applied for programming(writing) process, the transfer curves shifted toward the negative direction, as presented in Figure 2a and Figure S5 (Supporting Information). The programming operation impeded the formation of hole conductive channel because holes were transferred from pentacene and trapped into the Poly CD electret, leading to the shifts of transfer curves. Moreover, as the larger negative pulses were applied on the gate electrode, the greater shifts of the transfer curves could be obtained, which are summarized in Table 1. For transistor memory devices, memory window is a critical parameter defined as the difference in threshold voltages between the

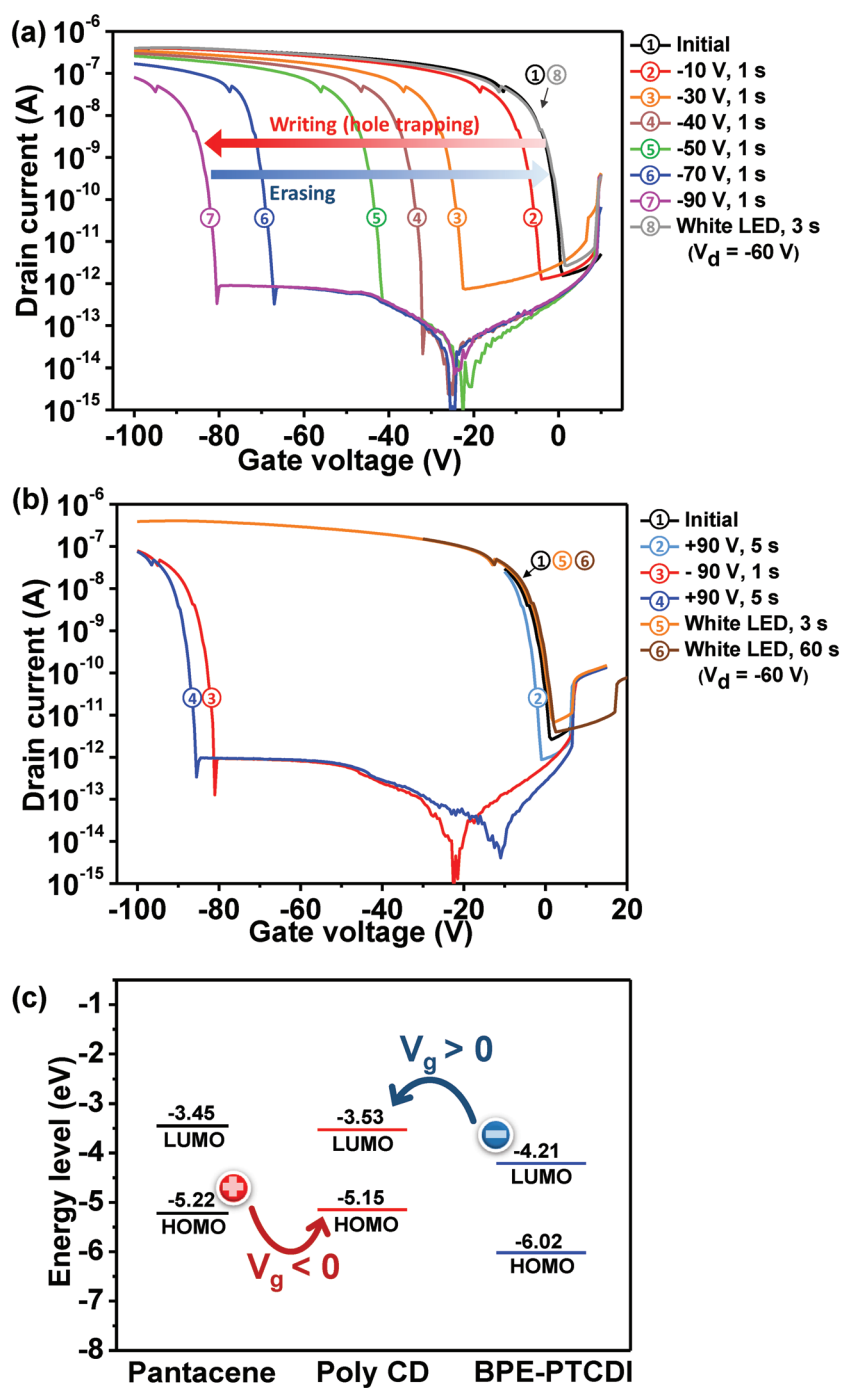


Figure 2. The memory characteristics of the p-type Poly CD based OFET memory devices a) operated by various negative applied gate pulses and b) in the electrical and optical operation mode by irradiating white LED light (25 mW). All currents were measured at the fixed drain voltage ($V_d = -60$ V) in the dark. c) The energy level diagram of organic semiconductors and Poly CD.

initial and programming traces. In Table 1, the maximum memory window of the Poly CD device could achieve a huge shift of 82 V, indicating an excellent hole-trapping capability. The increased shifts in the transfer curve upon application of different programming voltage stresses demonstrated that the trapping density of holes transferred from pentacene into the

Table 1. Summary of p-type Poly CD based OFET memory characteristic.

	Initial	-10 V, 1 s	-30 V, 1 s	-40 V, 1 s	-50 V, 1 s	-70 V, 1 s	-90 V, 1 s
Threshold voltage [V]	0	-5	-25	-35	-45	-68	-82
Memory window [V]	-	5	25	35	45	68	82
Memory behavior	Nonvolatile and nonerasable for electrical operation but photoerasable						

Poly CD electret is controllable. The effect of programming time on the shifts in the transfer curves was investigated and shown in Figure S6 (Supporting Information). The results suggested that 0.5 s for programming operation is sufficient for the detection of the well-defined shift. Intriguingly, the Poly CD memory devices exhibited irreversible switching behavior for positive electrical operation. It has been reported that the programmed devices would be erased through two paths, including the injection of opposite charges from the semiconductor and the detrapping of carriers from electret.^[1b,15] However, in the case of Poly CD, the electrically nonerasable behavior could be attributed to the design of Poly CD electret composed of 5,15-bis(2-decyltetradecyl)-9,19-difluoro-5,15-dihydrocarbazolo[3',4':5,6][1,4]oxazino[2,3-*b*]indolo[3,2-*h*]phenoxazine (Angular CD) with donor-acceptor moieties in a fully planar and conjugated fused-ring framework. The structure enabled to stabilize the injected charges through delocalization. In other words, due to the stabilization of the injected charges in the Angular CD moieties, the charges trapped in the electret cannot be released easily even under the reverse bias. The chemical nature of Poly CD generated a strong capturing ability for injected holes and thus resulted in the electrically nonerasable characteristic. Additionally, the dual sweep loops for programming and electrical erasing processes are depicted in Figure S7 (Supporting Information), however, both programming or erasing curves did not show obvious hysteresis phenomena. It suggested that the trapped holes could not fully be released due to the strong trapping ability^[16] nor be recombined with the injected electrons induced in the semiconductor layer.

2.3. Working Principle for “Photoinduced Recovery” Behavior

In order to investigate the mechanism of the photoinduced recovery of the Poly CD memory device, a series of experiments was designed. As shown in Figure 2b, the application of positive gate bias ($V_g = +90$ V, 5 s) after initial scan did not cause the memory effect, indicating that the Poly CD electret could not trap the electrons as p-type memory devices. The negative shift in the transfer curve then resulted when the programming operation ($V_g = -90$ V, 1 s) was applied representing the hole-trapping behavior. Due to the small difference, as shown in Figure 2c, in the highest occupied molecular orbital (HOMO) energy levels between Poly CD and pentacene, the holes induced on the HOMO energy level of pentacene could overcome the barrier at the interface and promote charge transfer to the Poly CD electret by the external electrical field. Subsequently, a reverse ($V_g = +90$ V, 5 s) bias was applied to the memory devices, serving as “electrical erasing process.” However, the transfer curve remained almost the same trace as the programmed transfer curve, implying that neither the trapped

holes extricate from Poly CD nor the electrons induced from pentacene recombine with the trapped holes by the electrical erasing operation. It is worth noting that the programmed devices, once exposed to white light, could be recovered to the initial state. Moreover, in spite of the longer exposure time, the transfer curve could only be similar to the originally initial state rather than shift toward the positive region (Figure 2b, line 1 and 6). On the basis of these results, we concluded that the p-type Poly CD based OFET memory devices could trap the holes only and possess the electrical nonerasable but photoerasable properties.

Herein, we proposed two possible mechanisms to interpret and comprehensively verify the photoinduced recovery behavior, as illustrated in Figure S8 (Supporting Information). In the previous studies, the guideline of applying organic semiconductors to a phototransistor was well-established.^[17] As organic semiconductors were illuminated by light, Frenkel excitons were generated and caused photocurrent.^[18] In the case of applying this phenomena to memory devices, the excitons would dissociate at the interface between the semiconductor and electret layers and the charges are then injected into the electret upon application of gate voltage stresses.^[19] In our case, one possible path to recovery was that the photoexcited electrons produced from pentacene are recombined with the trapped holes (Figure S8a, Supporting Information). The other possibility is that the photoinduced excitons generated in the Poly CD layer to recovery the device (Figure S8b, Supporting Information). To determine which mechanism path is more reasonable, the devices were exposed to light with specific wavelength. According to the results in UV-vis spectra, as shown in Figure 3a, the deposited pentacene film with the thickness of 50 nm hardly absorbed light at the wavelength of 365 nm, while the Poly CD film did. On the basis of the absorbance variation, if UV light (365 nm, 270 μ W) could also recover the programmed devices, the major factor in generating excitons for the photoinduced recovery behavior would be Poly CD rather than pentacene. As expected, the photoinduced recovery phenomena were also found by illuminating UV light (365 nm, 270 μ W) in Figure S9 (Supporting Information).

These results were ascribed to the photoresponse effect of Poly CD. The comprehensive mechanism is proposed and shown in Figure 3c. From the view point of chemical structure, Poly CD is composed of two donor carbazole moieties and dioxazine acceptor group. It is a common structure of donor-acceptor type organic sensitizers.^[20] Upon photoexcitation of the donor groups, the excited hole-electron pairs (excitons) were produced. To investigate the exciton dynamics, photoluminescence (PL) spectra were measured, as shown in Figure 3b. However, no noticeable peak was observed. On the basis of the UV-vis spectra in Figure 3a, Poly CD absorbed the light but no radiation occurred, the feature that is responsible

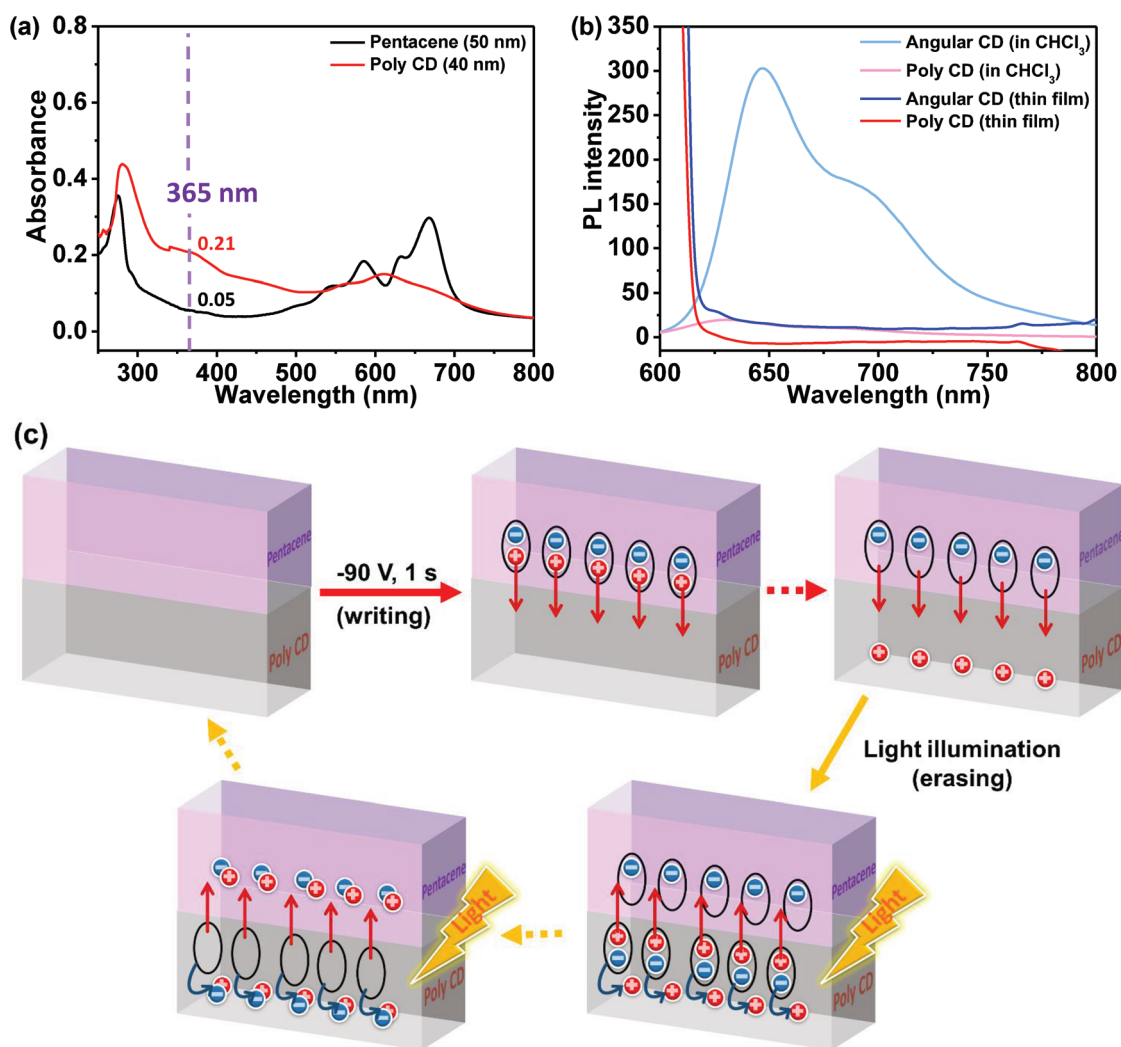


Figure 3. a) UV-vis spectra of Poly CD and pentacene with the thickness of 40 and 50 nm, respectively. b) Fluorescence spectra of Angular CD and Poly CD in film states (excited at 600 nm; Note that no emission was observed when excited at 500 nm) and in CHCl₃ solution (10^{-5} M repeat unit⁻¹, excited at 500 nm). The fluorescent quantum yields of Angular CD and Poly CD in CHCl₃ were 27.1 and 4.4%, respectively. c) Possible photoinduced recovery mechanism paths due to the excitons generated by Poly CD.

for the effective hole–electron pair separation.^[10] In this case, the delocalized excitons were generated after photoexcitation and the Coulombic interaction between the electron–hole pair decreased due to the interchain delocalization through the coplanar conjugated structure of the CD segment.^[21] The high energy electrons might effectively separate to eliminate the trapped holes, which served as electron acceptors in this condition, and the high energy holes transferred back to pentacene, finally leading to the photoinduced recovery behavior. To corroborate this explanation, we also fabricated the p-type OFET memory with polystyrene (PS)/Poly CD monomer (Angular CD) blended electret. PS as the matrix could reinforce the film-forming ability. Besides, the amount of PS was so low that the carriers could transfer from pentacene and be trapped into the electret via tunneling.^[22] The results are shown in Figure S10 (Supporting Information), which demonstrated the same photoinduced recovery properties and electrically nonerasable behavior as p-type Poly CD based OFET memory

devices. Therefore, it was confirmed that the photoinduced recovery phenomena are related to the highly planar CD structure homogeneously distributed in the smooth polymer matrix.

2.4. n-Type OFET Memory Employing Poly CD Electret

To verify the charge trapping mechanism, n-type Poly CD based OFET memory devices were also prepared by utilizing (*N,N'*-bis(2-phenylethyl)perylene-3,4,9,10-bis(dicarboximide) (BPE-PTCDI) as an n-type semiconductor. The AFM topography of the deposited BPE-PTCDI film overlying on the electret is shown in Figure S11 (Supporting Information), which presents a nanorod-like morphology. The output characteristics of the n-type Poly CD based OFET memory devices are shown in Figure S12 (Supporting Information).

Surprisingly, n-type Poly CD based OFET memory devices showed distinct properties from p-type ones. In Figure S13

(Supporting Information), the transfer curves could be triggered to shift toward the positive region by exerting the positive pulse of the gate bias, indicating the electron-trapping characteristics. The electrical erasing process (-90 V , 5 s) was also futile, exhibiting nonerasable characteristic. However, optical erasing process could recover the programmed devices, showing the similar photoinduced recovery behavior to the counter p-type device. In Figure 2c, the electron-trapping behavior could

be envisioned due to the alignments of LUMO energy levels at the interfaces between BPE-PTCDI and Poly CD. However, the inerasable property suggested that holes were insufficiently injected into the electret, which hindered the recombination with trapped electrons due to the significant difference between their HOMO energy levels. In regard to the results from p-type and n-type devices, it was interestingly found that the Poly CD exhibited ambipolar characteristics to trap holes or electrons

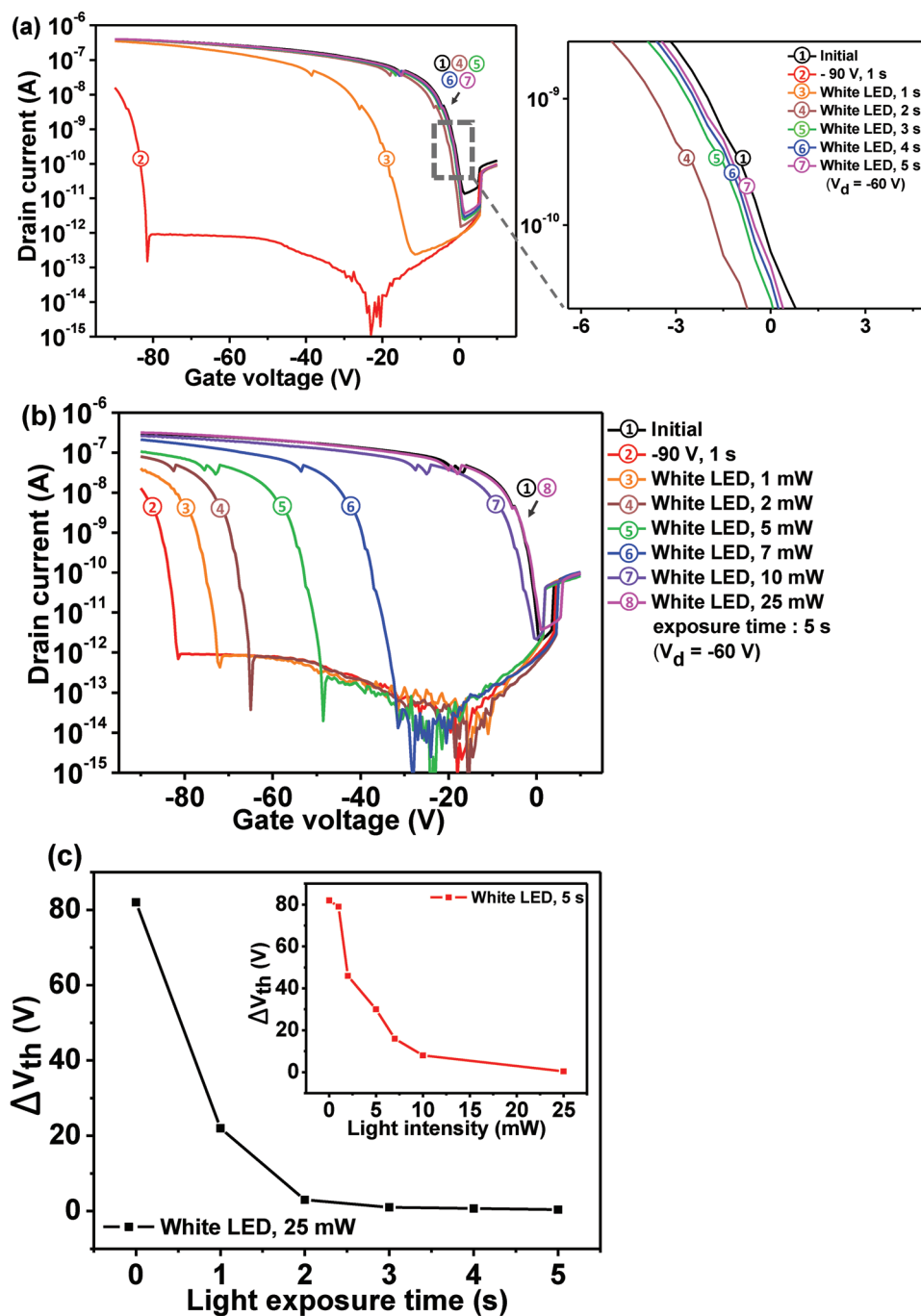


Figure 4. Photorecovery behavior of p-type Poly CD based OFET memory devices a) with various white LED light (25 mW) exposure time and b) various white LED light intensity for 5 s. c) The amount of threshold voltage shifts related to the light exposure time effect, and the light intensity effect as shown in the inset.

Table 2. Summary of the effect on light exposure time to recovery.

	Initial	−90 V, 1 s (program)	Light, 1 s ^{a)}	Light, 2 s ^{a)}	Light, 3 s ^{a)}	Light, 4 s ^{a)}	Light, 5 s ^{a)}
Threshold voltage [V]	0	−82	−22	−3	−1	−0.7	−0.4
Memory window [V]	0	82	22	3	1	0.7	0.4
Recovery ^{b)} [%]	100	0	73	96	99	99	100

^{a)}White LED light with intensity of 25 mW; ^{b)}Recovery = $(\Delta V_{th, program} - \Delta V_{th}) / (\Delta V_{th, program})$.

by employing different types of semiconductors, which were attributed to the donor–acceptor structure of the CD unit.^[23]

2.5. Application to Photorecorder

Since the OFET memory incorporated the photoinduced recovery feature, it was expected to be applicable to a photorecorder. In **Figure 4a**, the photoinduced recovery behavior was further investigated to look into the influence of exposure time, and the recovery percentage was evaluated by the formula listed in **Table 2**. The devices could be fully erased in 5 s, showing fast recovery response. Even for 2 s, the recovery percentage amounted up to 96%. The effect of exposure time on the recovery of n-type devices was also studied, as shown in **Figure S14** (Supporting Information). Accordingly, the effect of light intensity on the recovery behavior is summarized in **Figure 4b** and **Table 3**. The movements of memory window related to light exposure time and intensity are concluded in **Figure 4c**.

For practical applications of memory devices, retention characteristic is an important issue, referring to the data durability. If the devices could preserve the data without losing the trapped charges after removal of the applied power,^[1b] they serve as energy savings. Retention characteristics of the p-type Poly CD based OFET memories are recorded in **Figure 5a**. All current states could maintain stably over 10^4 s, indicating the nonvolatile nature. Here, the applied programmed voltage was set at −30 V for 1 s, suggesting that the Poly CD devices can work effectively even under a low voltage. For electrical operation, the devices could be defined as a write-one-read-many (WORM) type, nevertheless, by illumination of light for optical erasing operation, the WORM type devices could be converted into flash type, called photoresponsive flash memory.^[9a] The ratio of high-to-low currents, defined as memory ON/OFF ratio of the devices, showed more than 10^3 as the reading voltage was set at −10 V. This current ratio is distinguishable levels. Furthermore, the cyclic switching performances were also measured to evaluate the long-term durability, as

shown in **Figure 5b,c**. The durability tests were performed for 203 s cycle^{-1} , including 1 s-electrically programmed (−30 V) 100 s-reading, 2 s-light illumination, and 100 s-reading, and all currents were recorded at −10 V. As the result, the devices could reversibly switch without obvious decay after continuously 100 cycle measurements, which could meet the criteria of a photorecorder. Besides, we also practically made use of the devices to construct a photosensitive smart tag under dim light, as shown in **Figure S15** (Supporting Information). The devices were placed in an uncovered glove box to record the change of currents, and the fluorescent lights in the room outside the glove box were turned on. The light intensity measured near the devices was $10 \mu\text{W}$. Collectively speaking, the Poly CD based memory devices possessed reliability to stored data, and the photoresponsive characteristic could be further applied to photorecorder and photosensitive smart tag.

3. Conclusions

In summary, we developed photoresponsive flash memory devices based on newly synthesized polymer, Poly CD, as a charge-trapping layer. The polymer electret incorporated with p-type or n-type semiconductors showed an ambipolar nature in response to the variations of the trapped charges. However, the fast response of photoinduced recovery behavior could be observed in both p-type or n-type devices, attributed to the recombination of trapped charges and excitons generated in Poly CD. Furthermore, we proposed the coherence between the photoinduced recovery mechanism and chemical structure design. The effect of light exposure time and light intensity on the extent to recovery was also investigated, suggesting that the longer exposure time or the stronger intensity of light could result in the complete recovery. In addition, the Poly CD based memory devices exhibited nonvolatile characteristic over 10^4 s with high memory ratio of 10^3 and reliable durability under 100 continuous switching cycles, which provide the potential for use in photorecorder and photosensitive smart tag.

Table 3. Summary of the effect on light intensity to recovery.

	Initial	−90 V, 1 s (program)	Light, 1 mW ^{a)}	Light, 2 mW ^{a)}	Light, 5 mW ^{a)}	Light, 7 mW ^{a)}	Light, 10 mW ^{a)}	Light, 25 mW ^{a)}
Threshold voltage [V]	0	−82	−79	−46	−30	−16	−8	−0.4
Memory window [V]	0	82	79	46	30	16	8	0.4
Recovery ^{b)} [%]	100	0	4	44	63	80	90	100

^{a)}Every process of exposure time was kept for 5 s; ^{b)}Recovery = $(\Delta V_{th, program} - \Delta V_{th}) / (\Delta V_{th, program})$.

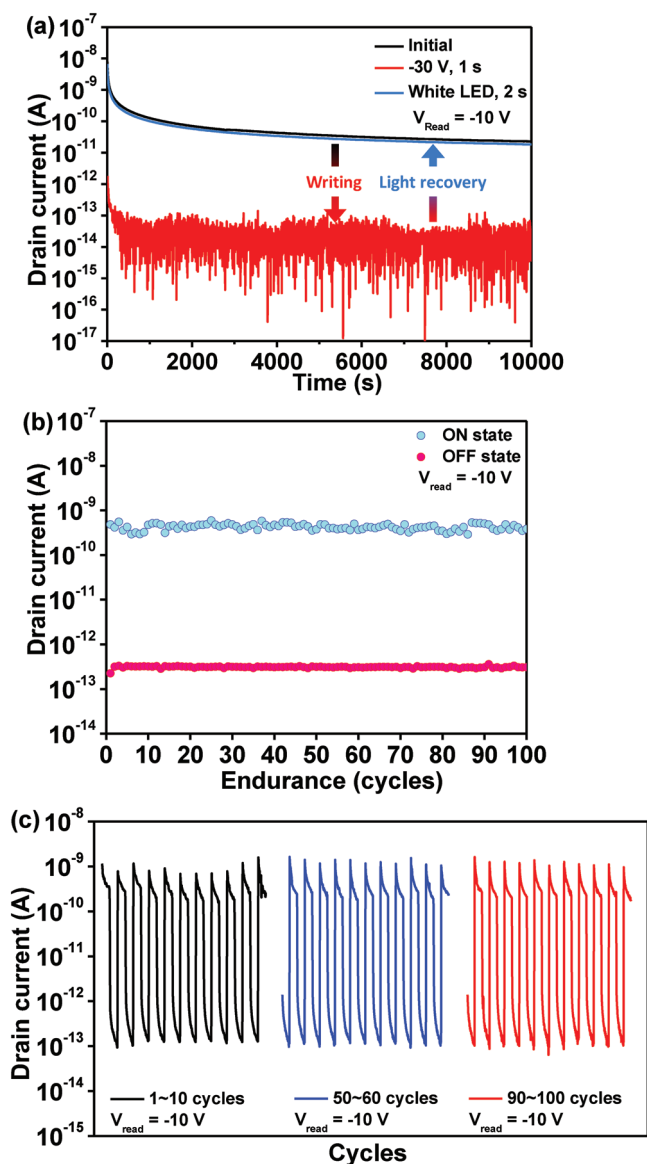


Figure 5. a) The retention characteristics before and after writing ($V_g = -30$ V)/light recovery operation. b) The 100 switching cycles durability test for photorecorder application of the p-type Poly CD based OFET memory devices. The measurements were conducted under dark environment. c) The expansion for 1–10, 50–60, and 90–100 cycles in (b). The switching test was performed for 203 s cycle⁻¹, including 1 s-electrically programmed ($V_g = -30$ V) 100 s-reading, 2 s-light illumination (25 mW), and 100 s-reading, and all currents were recorded at -10 V.

4. Experimental Section

Materials: Angular CD was synthesized according to the reported procedure,^[12] as shown in Scheme S1 (Supporting Information). Other reagents were used as received.

Synthesis of Poly CD: To a solution of bisphenol A (0.030 g, 0.12 mmol) in NMP (5 mL), K_2CO_3 (0.030 g, 0.19 mmol) and toluene (5 mL) were added. The mixture was heated to 140 °C for 3 h to remove water. After cooling to room temperature, Angular CD (0.10 g, 0.12 mmol) was added and the mixture was stirred at 180 °C for 20 h. The mixture was cooled down to room temperature and poured into methanol. The green precipitate was collected and dried in vacuo, which was followed

by Soxhlet washing with methanol (78 mg, 46%). The synthetic route is shown in Figure 1. GPC (THF): M_w 4000, M_n 3300; 1H NMR (300 MHz, C_6D_6 , δ): 0.8–2.1 (m, 100 nH), 4.0–4.2 (br, 4 nH), 6.5–7.7 ppm (m, 20 nH); IR (neat): $\nu = 2921.6, 2852.2, 1699.0, 1683.6, 1634.4, 1602.6, 1507.1, 1487.8, 1457.9, 1376.9, 1336.4, 1210.1, 1177.3, 1140.0, 1108.9, 1017.3, 830.2, 799.4, 721.2$ cm⁻¹.

Thin Film Preparation, Device Fabrication: Classic OFET memory devices were fabricated on a heavily n-type Si wafer with a 300 nm thick SiO_2 dielectric layer in a bottom-gate/top-contact configuration. The wafer was precleaned with solvent procedure. The chlorobenzene solution of Poly CD at the concentration of 10 mg mL⁻¹ was filtered with a polytetrafluoroethylene membrane syringe filter (pore size, 0.22 μ m) and then spin-coated on the precleaned wafer at a rotation speed of 3000 rpm for 1 min. After that, the polymer film was annealed at 120 °C for 1 h. The thickness of the electrets in the study was controlled at 40 nm. The pentacene or BPE-PTCDI layer (50 nm) was fabricated on the electret by vacuum deposition at the growth rate of 0.3 Å s⁻¹ under 10⁻⁷ torr at room temperature. The top-contact source–drain gold electrode (60 nm) was successively deposited on the semiconductor layer at the rate of 0.5 Å s⁻¹ through a shadow mask with the channel length (L) and width of 50 μ m and 1000 μ m, respectively.

Measurement and Characterization: The properties of OFET memories were measured by a Keithley 4200-SCS semiconductor parameter analyzer at room temperature in an inert atmosphere glove box. The surface structures of the semiconductors and electrets were measured by a Nanoscope 3D controller AFM operated in the tapping mode at room temperature. Spectroscopic reflectometer (Filmetrics F20) was used to precisely determine the thickness of electrets. The contact angles were measured by a First-Ten-Angstroms FTA-1000B instrument with drops of pure water. Cyclic voltammetry (CV) measurements were performed by a BAS electrochemical analyzer model 612C at room temperature in a classical three-electrode cell with a sweep rate of 0.1 V s⁻¹. The working, reference, and auxiliary electrodes were a glassy carbon electrode, Ag/AgNO₃/CH₃CN/(*n*-C₄H₉)₄NClO₄, and Pt wire, respectively. Polymer films were drop-cast onto the working electrode from ≈ 2 mg mL⁻¹ of the sample solutions in chloroform. For calibration, the redox potential of ferrocene/ferrocenium (Fc/Fc⁺) was measured under the same conditions, and it was located at 0.09 V versus the Ag/AgNO₃ electrode. It was assumed that the redox potential of Fc/Fc⁺ has an absolute energy level of -4.80 eV to vacuum. The HOMO and LUMO energy levels were then calculated according to the following equations

$$E_{HOMO} = -(\varphi_{ox} + 4.71) [eV] \quad (1)$$

$$E_{LUMO} = -(\varphi_{red} + 4.71) [eV] \quad (2)$$

where φ_{ox} is the onset of the oxidation peak and φ_{red} is the onset of the reduction peak.

Fourier transform infrared (FTIR) spectra were recorded on a JASCO FT/IR-4100 spectrometer in the range from 4000 to 600 cm⁻¹. UV–vis spectra were recorded by a JASCO V-670 spectrophotometer for solutions in CHCl₃ or thin films deposited on a glass substrate. The PL spectra were measured by a JASCO FP-6500 spectrofluorometer. Film thicknesses were measured by a KLA-Tencor Alpha-Step D-100 stylus profiler. GPC was measured by a JASCO GULLIVER 1500 equipped with the pump (PU-2080 Plus), absorbance detector (RI-2031 Plus), and two Shodex GPC KF-803 columns (8.0 mm I.D. \times 300 mm L) at 40 °C. The flow rate was 1.0 mL min⁻¹ for the THF eluent. The molecular weights were calculated based on the calibration curves using polystyrene standards.

1H NMR spectra were recorded by a JEOL AL-300 (300 MHz) spectrometer at room temperature. Deuterated benzene (C_6D_6) and chloroform ($CDCl_3$) were used as the solvent and the chemical shifts were reported in parts per million (ppm) relative to the reference TMS peak at 0 ppm. Coupling constants J were given in Hertz. The resonance multiplicity was described as singlet (s), doublet (d), triplet (t), multiplet (m), and broadening (br).

Supporting Information

Supporting Information is available from the Wiley Online Library or from the author.

Acknowledgements

C.-H.C. and Y.W. contributed equally to this work. This work was financially supported by the "Advanced Research Center for Green Materials Science and Technology" from the Featured Area Research Center Program within the framework of the Higher Education Sprout Project by the Ministry of Education (108L9006) and the Ministry of Science and Technology in Taiwan (MOST 108-3017-F-002-002, 107-2113-M-002-024-MY3, and 107-2221-E-002-066-MY3) as well as JSPS KAKENHI (Grant No. 19H02786), the Ogasawara Foundation for the Promotion of Science and Engineering, the Yazaki Memorial Foundation for Science and Technology, and the Asahi Glass Foundation.

Conflict of Interest

The authors declare no conflict of interest.

Keywords

ambipolar, optical memory, organic field-effect transistor memory, photoinduced recovery, polymer electret

Received: April 13, 2019

Revised: June 17, 2019

Published online: August 8, 2019

- [1] a) S. T. Han, Y. Zhou, V. Roy, *Adv. Mater.* **2013**, *25*, 5425; b) Y.-H. Chou, H.-C. Chang, C.-L. Liu, W.-C. Chen, *Polym. Chem.* **2015**, *6*, 341; c) T. Leydecker, M. Herder, E. Pavlica, G. Bratina, S. Hecht, E. Orgiu, P. Samorì, *Nat. Nanotechnol.* **2016**, *11*, 769.
- [2] a) S. J. Kang, Y. J. Park, I. Bae, K. J. Kim, H. C. Kim, S. Bauer, E. L. Thomas, C. Park, *Adv. Funct. Mater.* **2009**, *19*, 2812; b) D. Thuau, M. Abbas, G. Wantz, L. Hirsch, I. Dufour, C. Ayela, *Org. Electron.* **2017**, *40*, 30.
- [3] a) K. J. Baeg, Y. Y. Noh, H. Sirringhaus, D. Y. Kim, *Adv. Funct. Mater.* **2010**, *20*, 224; b) S.-J. Kim, Y.-S. Park, S.-H. Lyu, J.-S. Lee, *Appl. Phys. Lett.* **2010**, *96*, 7.
- [4] a) K. J. Baeg, Y. Y. Noh, J. Ghim, S. J. Kang, H. Lee, D. Y. Kim, *Adv. Mater.* **2006**, *18*, 3179; b) T. B. Singh, N. Marjanović, G. Matt, N. Sariciftci, R. Schwödiauer, S. Bauer, *Appl. Phys. Lett.* **2004**, *85*, 5409.
- [5] a) M. Yi, M. Xie, Y. Shao, W. Li, H. Ling, L. Xie, T. Yang, Q. Fan, J. Zhu, W. Huang, *J. Mater. Chem. C* **2015**, *3*, 5220; b) M.-Y. Chiu, C.-C. Chen, J.-T. Sheu, K.-H. Wei, *Org. Electron.* **2009**, *10*, 769; c) X. Gao, C.-H. Liu, X.-J. She, Q.-L. Li, J. Liu, S.-D. Wang, *Org. Electron.* **2014**, *15*, 2486; d) S.-W. Cheng, T. Han, T.-Y. Huang, Y.-H. C. Chien, C.-L. Liu, B. Z. Tang, G.-S. Liou, *ACS Appl. Mater. Interfaces* **2018**, *10*, 18281; e) Y. Guo, C.-a. Di, S. Ye, X. Sun, J. Zheng, Y. Wen, W. Wu, G. Yu, Y. Liu, *Adv. Mater.* **2009**, *21*, 1954.
- [6] a) C. Sun, Z. Lin, W. Xu, L. Xie, H. Ling, M. Chen, J. Wang, Y. Wei, M. Yi, W. Huang, *J. Phys. Chem. C* **2015**, *119*, 18014; b) W. Li, F. Guo, H. Ling, H. Liu, M. Yi, P. Zhang, W. Wang, L. Xie, W. Huang, *Small* **2018**, *14*, 1701437.
- [7] a) S.-W. Cheng, T. Han, T.-Y. Huang, Y.-H. C. Chien, C.-L. Liu, B. Z. Tang, G.-S. Liou, *ACS Appl. Mater. Interfaces* **2018**, *10*, 18281; b) S.-T. Han, Y. Zhou, L. Zhou, Y. Yan, L.-B. Huang, W. Wu, V. A. L. Roy, *J. Mater. Chem. C* **2015**, *3*, 3173.
- [8] a) Y. Wang, E. Liu, A. Gao, T. Cao, M. Long, C. Pan, L. Zhang, J. Zeng, C. Wang, W. Hu, S.-J. Liang, F. Miao, *ACS Nano* **2018**, *12*, 9513; b) M. D. Tran, H. Kim, J. S. Kim, M. H. Doan, T. K. Chau, Q. A. Vu, J.-H. Kim, Y. H. Lee, *Adv. Mater.* **2019**, *31*, 1807075.
- [9] a) Y. J. Jeong, D.-J. Yun, S. H. Kim, C. E. Park, J. Jang, *ACS Nano* **2018**, *12*, 7701; b) Y. J. Jeong, D.-J. Yun, S. H. Kim, J. Jang, C. E. Park, *ACS Appl. Mater. Interfaces* **2017**, *9*, 11759.
- [10] N. A. Nisamy, K. I. Jayawardena, A. D. T. Adikaari, S. R. P. Silva, *Adv. Mater.* **2011**, *23*, 3796.
- [11] a) Y.-H. Chou, S. Takasugi, R. Goseki, T. Ishizone, W.-C. Chen, *Polym. Chem.* **2014**, *5*, 1063; b) J.-C. Hsu, W.-Y. Lee, H.-C. Wu, K. Sugiyama, A. Hirao, W.-C. Chen, *J. Mater. Chem.* **2012**, *22*, 5820; c) Z. Hu, E. Reichmanis, *J. Polym. Sci., Part A: Polym. Chem.* **2011**, *49*, 1155.
- [12] H. Tatsumi, Y. Wang, Y. Aizawa, M. Tokita, T. Mori, T. Michinobu, *J. Phys. Chem. C* **2016**, *120*, 26686.
- [13] a) H. Yang, S. H. Kim, L. Yang, S. Y. Yang, C. E. Park, *Adv. Mater.* **2007**, *19*, 2868; b) W.-Y. Chou, C.-W. Kuo, H.-L. Cheng, Y.-R. Chen, F.-C. Tang, F.-Y. Yang, D.-Y. Shu, C.-C. Liao, *Appl. Phys. Lett.* **2006**, *89*, 112126.
- [14] Y.-C. Chiu, C.-C. Shih, W.-C. Chen, *J. Mater. Chem. C* **2015**, *3*, 551.
- [15] a) K.-J. Baeg, Y.-Y. Noh, J. Ghim, B. Lim, D.-Y. Kim, *Adv. Funct. Mater.* **2008**, *18*, 3678; b) Y.-C. Chiu, C.-L. Liu, W.-Y. Lee, Y. Chen, T. Kakuchi, W.-C. Chen, *NPG Asia Mater.* **2013**, *5*, e35.
- [16] a) T. Kim, J. W. Lim, S. H. Lee, J. Na, J. Jeong, K. H. Jung, G. Kim, S. J. Yun, *ACS Appl. Mater. Interfaces* **2018**, *10*, 26405; b) Y.-F. Wang, M.-R. Tsai, P.-Y. Wang, C.-Y. Lin, H.-L. Cheng, F.-C. Tang, S. L.-C. Hsu, C.-C. Hsu, W.-Y. Chou, *RSC Adv.* **2016**, *6*, 77735.
- [17] a) X. Liu, G. Dong, L. Duan, L. Wang, Y. Qiu, *J. Mater. Chem.* **2012**, *22*, 11836; b) B. Park, K. Whitham, J. Cho, E. Reichmanis, *ACS Nano* **2012**, *6*, 9466.
- [18] O. Ostroverkhova, *Chem. Rev.* **2016**, *116*, 13279.
- [19] Y. Zhai, J.-Q. Yang, Y. Zhou, J.-Y. Mao, Y. Ren, V. A. Roy, S.-T. Han, *Mater. Horiz.* **2018**, *5*, 641.
- [20] a) S. M. J. Nabavi, B. Hosseinzadeh, M. Tajbakhsh, H. Alinezhad, *J. Mater. Sci.: Mater. Electron.* **2018**, *29*, 3270; b) X. Zhang, Y. Xu, F. Giordano, M. Schreier, N. Pellet, Y. Hu, C. Yi, N. Robertson, J. Hua, S. M. Zakeeruddin, *J. Am. Chem. Soc.* **2016**, *138*, 10742.
- [21] K. H. Park, W. Kim, J. Yang, D. Kim, *Chem. Soc. Rev.* **2018**, *47*, 4279.
- [22] C. C. Shih, Y. C. Chiu, W. Y. Lee, J. Y. Chen, W. C. Chen, *Adv. Funct. Mater.* **2015**, *25*, 1511.
- [23] A. Benito-Hernández, M. T. El-Sayed, J. T. L. Navarrete, M. C. R. Delgado, B. Gómez-Lor, *Org. Chem. Front.* **2018**, *5*, 1748.